DOI: 10.1002/chem.200900825

Electrochemical Characterisation of 6-Iodomaltose, 6′-Iodomaltose and 6-Iodomaltotriose on a Silver Cathode and Their One-Pot Electrochemical Dimerisation to New Mixed O/C Maltotetraose and Maltohexaose Mimics

Angelo Alberti,[b] Dante Macciantelli,[b] Annamaria Naggi,[c] Elena Urso,[c] Giangiacomo Torri,[c] and Elena Vismara*[a]

Dedicated to the Centenary of the Italian Chemical Society

Abstract: The electrochemical reduction on silver of peracetylated 6-iodo-6-deoxy-β-maltose (**2**), 6-iodo-6-deoxy-β-maltotriose (**3**) and 6′-iodo-6′-deoxy-β-maltose (**4**) has been investigated by cyclic voltammetry and performed on a preparative scale, according to the stoichiometry, $-CH_2I(\mathbf{2}–\mathbf{4}) + e^- \rightarrow -CH_2^{\bullet} + I^-$. In agreement with the preparative electrolysis results, cyclic voltammetry showed different profiles for the reducing terminal-iodinated **2** and **3** and for the non-reducing terminal-iodinated **4**. Compounds **2** and **3** partly dimerised to maltotetraoses mimics **7** (6,6-dimer) and **8** (5′,5′-dimer) in 38% overall yield and to maltohexaose mimics **12** (6,6-dimer) and **13** (5′,5′-dimer) in 30% overall yield, respectively. Compounds **7** and **12** came from the dimerisation of $-CH_2^{\bullet}$, primary radicals at C-6, which could also abstract H-5′, becoming CH_3 and generating the C-5′ quaternary radicals that dimerised in **8** and **13**, respectively. These products were accompanied by the maltose derivatives **9**, **10** and **11a/b** in 42% overall yield and by the maltotriose derivatives **14**, **15** and **16** in 48% overall yield, respectively. Compounds **9**, **14** and **10**, **15** came from $-CH_2^{\bullet}$ disproportionation to CH_3 and CH_2=C, respectively (exocyclic double bond C-6/C-5). Compounds **11a/b** and **16** came from C-5′ radical reduction, followed by acetate anion elimination (double bonds C-6′/C-5′ and C-5′/C-4′). In turn, **4** afforded only the 6′,6′-dimer maltotetraose mimic **17** in 60% yield, accompanied by the reduced maltose **18** in 20% yield, in which the starting CH_2I became CH_3. Compounds **7**, **8**, **12**, **13** and **17** belong to a class of mixed O/C malto-mimic oligosaccharides wherein an unnatural C–C bond between two saccharide units increases metabolic stability compared to their O-analogues and modulates the sugar chain conformational flexibility, a fundamental parameter in determining protein–carbohydrate binding. Direct and spin-trapping EPR studies substantiated the radical-based nature of the dimerisation processes and allowed the identification of some of the paramagnetic species involved.

Keywords: carbohydrates · electrochemistry · maltomimics · radicals · silver

Introduction

The electroreduction of halosaccharides on a silver cathode is a well-established technique providing a mild, clean and one-pot method for the preparation of double sugar units through the formation of stable interglycosidic C–C bonds. More precisely, it is a synthetic procedure whereby dimerisation of a carbon-centred radical follows the loss of a halide anion from an electrochemically reduced halo sugar and affords C-disaccharide mimics (see Scheme 1),[1–3] mixed O/C-maltotetraose mimics from acetobromomaltose (ABM)[4] and mixed O/C-maltohexaose mimics from acetobromomaltotriose (ABMT;[5] see Scheme 2).

Actually, it should be emphasised that the real bioactive moieties of natural polysaccharides are specific or unspecific

[a] Prof. Dr. E. Vismara
Dipartimento di Chimica
Materiali et Ingegneria Chimica "G. Natta"
Politecnico di Milano (Italy)
Fax: (+39) 0223993180/3080
E-mail: elena.vismara@polimi.it

[b] Dr. A. Alberti, D. Macciantelli
ISOF-CNR Area di Ricerca
via Pietro Gobetti 101, 40129 Bologna (Italy)

[c] Dr. A. Naggi, Dr. E. Urso, Dr. G. Torri
Istituto di Ricerche Chimiche e Biochimiche "G. Ronzoni"
via Giuseppe Colombo 81, 20133 Milano (Italy)

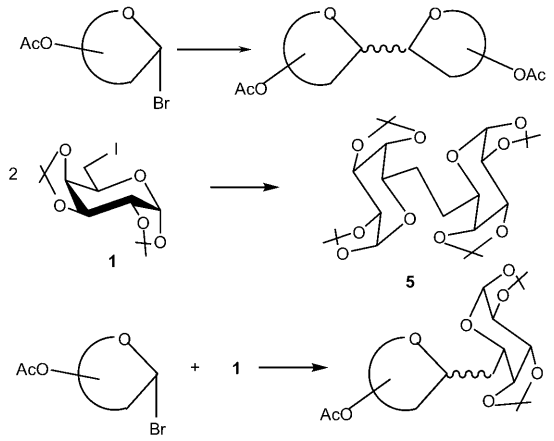

Scheme 1. Halo-monosaccharide electroreduction derivatives.

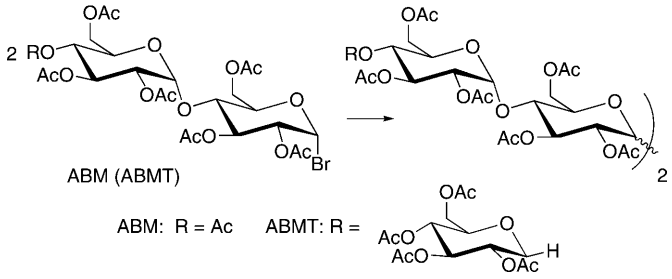

Scheme 2. ABM and ABMT electroreduction derivatives.

oligosaccharides of more than four sugar units.[6] Due to their small molecular size, oligosaccharides show a larger bioavailability than their polymeric precursors. As a result, large efforts have been addressed to preparing synthetic oligosaccharides that may mimic the natural ones.

In recent years, we have begun focussing our attention on linear malto-oligosaccharides, especially on maltohexaose, whose sulfated forms have been found to be efficient inhibitors of tumour growth and metastasis.[7] We then moved to building up mixed O/C-malto-oligosaccharides and checking whether or not their sulfated forms would mimic natural malto-oligosaccharide. The sugar chains of these mimics are characterised by the presence of an interglycosidic C–C bond that is expected to induce chemical and metabolic stability with respect to malto-oligosaccharides, similarly to what has been observed for C-glycosides that are less vulnerable to metabolic processing than their O-analogues and for this reason have been studied as drug candidates and inhibitors of carbohydrate-processing enzymes.[8] The presence of the interglycosidic C–C bond is an important feature because, as shown by a molecular modelling conformational analysis,[5] it modifies the geometry of the sugar chains and makes their conformation rigid. In fact, the conformational flexibility of oligosaccharides is critical in determining their binding to protein and consequently their bioactivity.[9] The majority of oligosaccharides are flexible, which allows them to assume proper conformations to adapt themselves to the binding site of a specific protein (favourable enthalpic contribution). However, the binding brings along an unfavourable entropy contribution, because it reduces the flexibility of the oligosaccharide. Thus, although high flexibility of oligosaccharides helps the binding, too much flexibility may hamper the carbohydrate–protein complex formation. To gain an understanding of structure/activity relationships of natural and synthetic carbohydrate-based structures, many studies were done in various directions: these include modelling protein recognition of carbohydrates,[10] simulating and modelling flexible sugar rings,[11] synthesising conformationally constrained oligosaccharides,[12] comparing C-glycoside and O-glycoside conformation[13] and more recently developing multidisciplinary approaches to the study of protein–carbohydrate complexes, made possible by the technical developments in NMR spectroscopy and X-ray diffraction.[14] Nevertheless, despite all these activities, this understanding seems a long way from being achieved. The most important property of the sulfated forms of the O/C-maltohexaose mimics reported in Scheme 2 is that, in addition to the above features, they are biologically active and have a real chance of being developed as new carbohydrate-based drugs having anti-tumour and anti-metastatic activities.[15]

These positive results prompted us to prepare different "malto-mimics" by strategically choosing the position of the halogen atom in the starting halo sugar. Thus, we have endeavoured in the preparation of new structures derived from the coupling of iodomaltose and iodomaltotriose in which the iodine atom is bound to the exocyclic carbon of either the reducing or non-reducing-sugar end unit.

We report here on the outcome of the electrochemical reduction of the model compound 1,2:3,4-di-*O*-isopropylidene-6-deoxy-6-iodo-α-D-galactose (**1**),[3,16] of 1,2,3,2′,3′,4′,6′-hepta-*O*-acetyl-6-deoxy-6-iodo-β-maltose (**2**),[17] 1,2,3,2′,3′,6′,2″,3″,4″,6″-deca-*O*-acetyl-6-deoxy-6-iodo-β-maltotriose (**3**)[18] and 1,2,3,6,2′,3′,4′-hepta-*O*-acetyl-6′-deoxy-6′-iodo-β-maltose (**4**).[17]

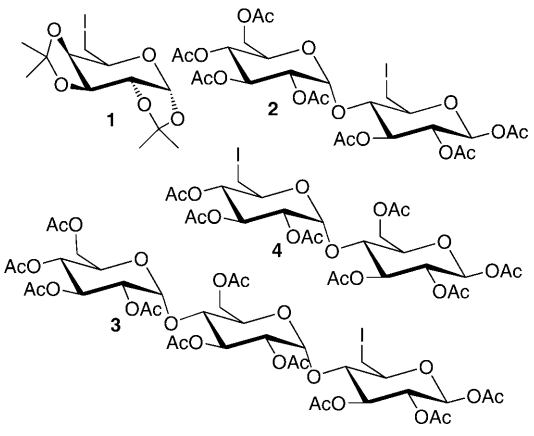

Results

Cyclic voltammetry: The cyclic voltammetry on a silver cathode of compounds **1**–**4** in acetonitrile was explored at different sweep rates prior to carrying out the preparative electrolysis.

Complex and irreversible voltammograms consisting of several waves were observed in all cases, their relative intensities being dependent on the sweep rate.

Compounds **1** and **4** exhibit similar trends. At scan rates $\leq 200\ mV\,s^{-1}$ a first reduction wave at approximately -1.15 to -1.25 V and a broad second wave at higher potentials (ca. -1.78 V for **1** and between -1.5 and -1.85 V for **4**) are observed, with the former wave corresponding to the reduction of the carbon–iodine bond. At $500\ mV\,s^{-1}$, **4** exhibits a unique second wave between -1.3 and -1.9 V, whereas for **1** the two waves begin to be superimposed although still distinguishable. At $800\ mV\,s^{-1}$ only one broad band is visible for both **1** and **4**. In the voltammograms of **2** and **3**, the reduction wave of the carbon–iodine bond around -1.2 V is accompanied by a second wave very close to the first and a third wave at more negative potentials. The second wave is very weak, in fact hardly visible at scan rates $\leq 50\ mV\,s^{-1}$, but becomes more and more relevant as the scan rate grows faster (from 50 to $500\ mV\,s^{-1}$) while the first wave loses intensity, shifting slightly to more negative potentials. In the same scan range, the third wave shifts from 1.56 to 1.99 V. At $800\ mV\,s^{-1}$ only the second wave remains visible in the interval between 0 and -2.3 V, the third wave having probably shifted beyond -2.5 V.

This is evidenced in Figure 1, in which the forward reduction voltammograms are shown for compounds **1**, **2** and **4** (the voltammogram observed for **3** is virtually identical to that observed for **2**).

After the first scan, small waves are also detected for all sugars in the interval between 0 and -0.7 V. These are due to the reduction of the iodine released as iodide anion from the sugar after the first reduction.

Preparative electrolysis experiments: Potentiostatic electrolyses were carried out in acetonitrile in a two-compartment cell, with the cathode and anode both being silver plates.

Electrolysis details, workup and product isolations have been detailed in the Experimental Section. The isolated products can be divided in two classes: dimers, that is, compounds that have twice the number of sugar units of the starting compound, and thus twice the molecular weight of the intermediate radicals resulting from the loss of the iodine anion (see Scheme 3), and compounds that have the same number of sugar units as the starting compound and thus a molecular weight close to that of the intermediate radical (see Scheme 4).

In Table 1 we report their quantitative yields. Compounds **1** and **4** exhibit similar trends. Compound **1** was reduced to the C-disaccharide mimic **5**,[3] and to the galactose derivative **6**.[16] Compound **4** afforded only the 6′,6′-dimer maltotetraose mimic **17** accompanied by the maltose derivative

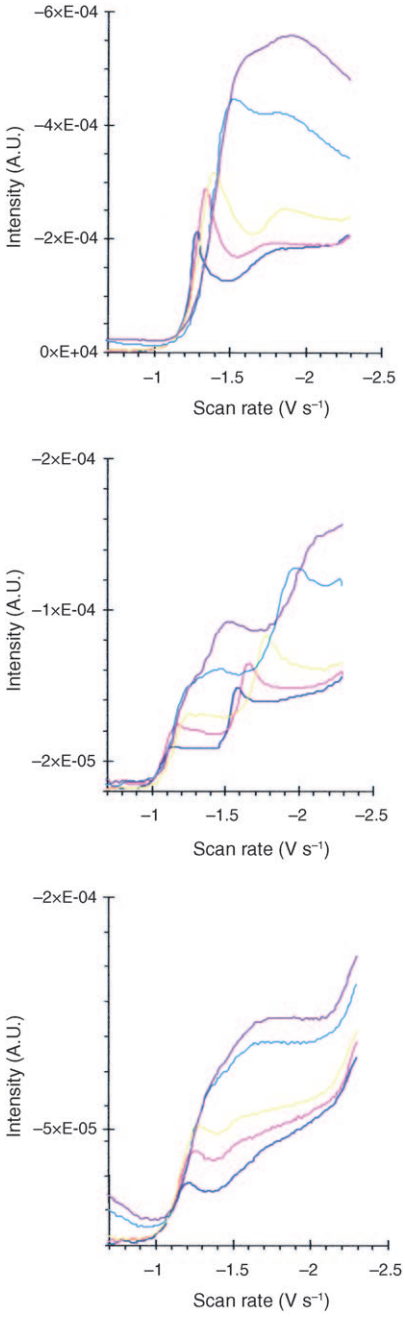

Figure 1. Forward cyclovoltammetric reduction traces for compounds top) **1**, middel) **2** and bottom) **4**. Scan rates are 50 (black), 100 (red), 200 (yellow), 500 (blue) and 800 (purple) $mV\,s^{-1}$.

18.[17,19] In turn, **2** and **3** partly dimerised to maltotetraoses mimics **7** (6,6-dimer) and **8** (5′,5′-dimer) and to maltohexaose mimics **12** (6,6-dimer) and **13** (5′,5′-dimer), respectively. These products were accompanied by the maltose derivatives **9**,[19] **10**[20] and **11a/b**, and by the maltotriose derivatives **14**, **15**[18] and **16**, respectively.

The maintenance of the C5′ D-glucose configuration and conformation in **8** and **13** was supported by optical rotation and NMR spectroscopic characterisation, as detailed in the Experimental Section. The alternative L-ido configuration is

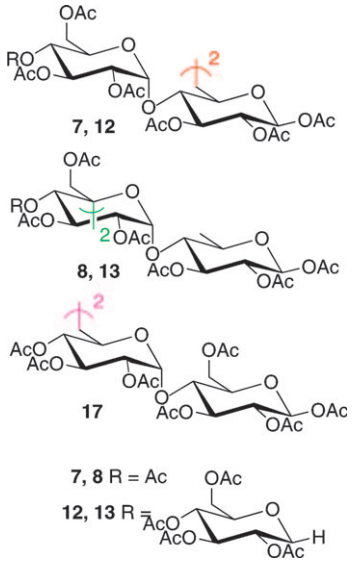

Scheme 3. Dimerisation derivatives isolated in the preparative electrolysis of compounds **2**–**4**.

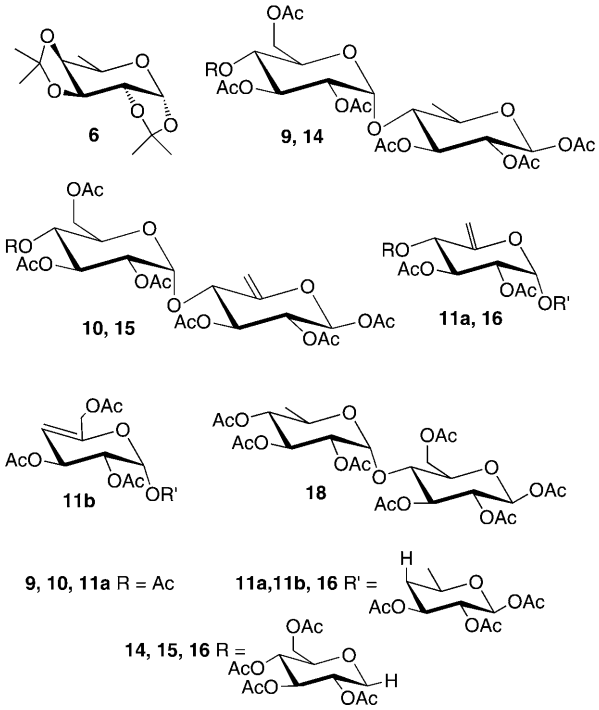

Scheme 4. Reduction, disproportionation and rearrangement derivatives isolated upon preparative electrolysis of compounds **1**–**4**.

Table 1. Product distribution in the preparative electrolysis of sugars **1**–**4**.

	Yield[a]	Yield[a]	Yield[a]	Yield[a]	Yield[a]
1[b]	–	71 (**5**)	15 (**6**)	–	–
2	29 (**7**)	9 (**8**)	–	12 (**9**,**10**)	30 (**11a/b**)
3	18 (**12**)	12 (**13**)	–	24 (**14**,**15**)	24 (**16**)
4	–	60 (**17**)	20 (**18**)	–	–

[a] % yield of the isolated compound that is given in parentheses. [b] Data from ref. [3].

expected to contribute with negative optical rotation (α) values.[21] Preliminary semi-empirical (AM1) calculations on **13** were also performed and elucidated the C_2 symmetry (see Figure 2).

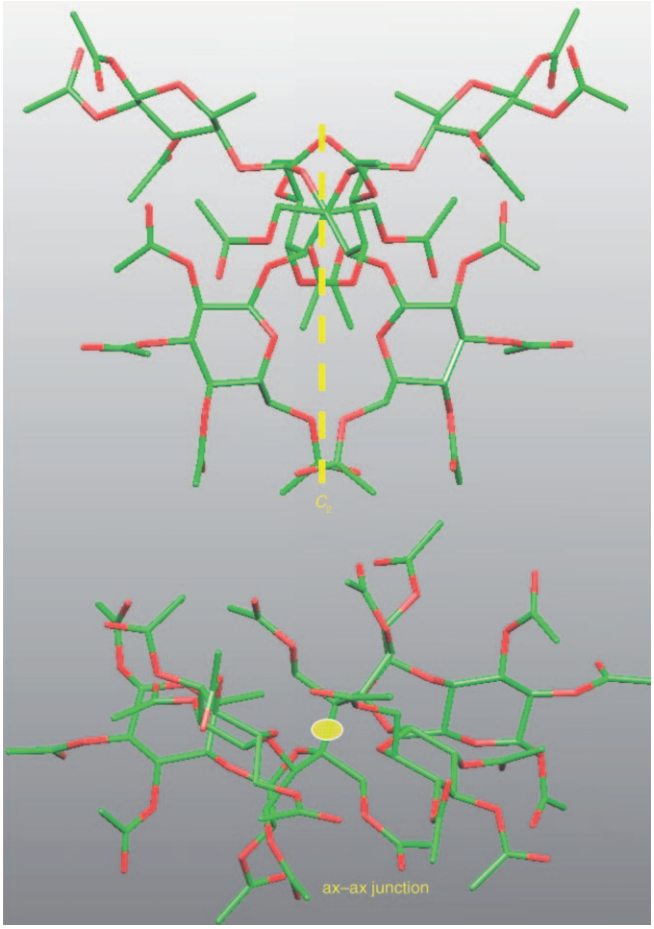

Figure 2. Molecular modelling geometry of compound **13**.

EPR spectroscopy: Although the first step of the electroreduction of the investigated iodo-sugars is conceivably the formation of the corresponding radical anions that immediately undergo loss of an iodide anion with formation of the corresponding 6-yl primary radicals, no EPR spectra could be observed upon room-temperature electrochemical reduction of sugars **1**–**4** inside the cavity of the EPR spectrometer.

This was attributed to a very low persistence of the resulting radicals. Indeed, the persistence of these paramagnetic species should increase at low temperature, but our equipment setup did not allow low-temperature electrochemical EPR experiments. Therefore, the generation of the 6-yl primary radicals from **1**–**4** at low temperature was attempted by iodine abstraction (see Experimental Section).

Figure 3a shows the EPR spectrum observed by irradiating with UV light at $T=-70\,^{\circ}C$ a thoroughly degassed solu-

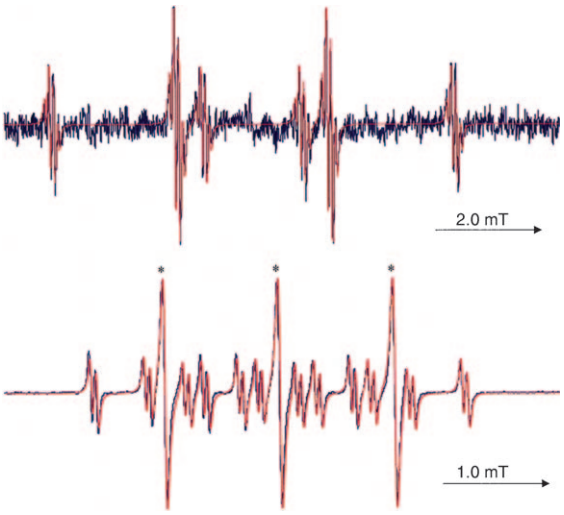

Figure 3. EPR spectra observed upon photolysis of a degassed solution of **1** and hexabutylditin in cyclopropane (top) and a degassed solution of **1**, hexabutylditin and MNP in cyclopropane (bottom). The lines marked with * are due to di-*tert*-butyl nitroxide. Experimental traces are in blue, computer-reproduced traces in red.

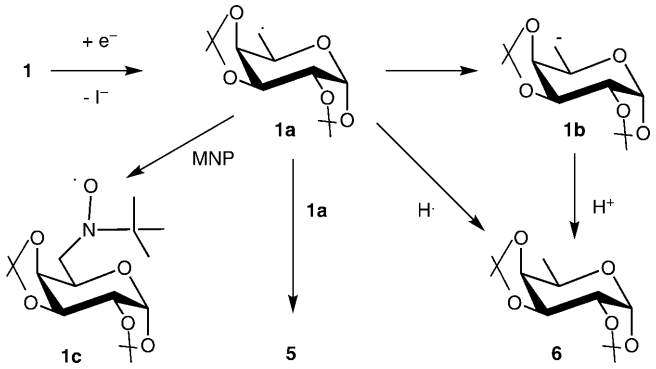

Scheme 5. Generation of **1a**, MNP trapping (**1c**), dimerisation (**5**) and reduction (**6**).

tion of sugar **1** in cyclopropane containing a small amount of hexabutylditin.

On the basis of the spectral parameters (see Table 2),[22] the spectrum can be safely attributed to radical **1a**, with the two methylenic hydrogen atoms being responsible for the 2.414 mT triplet and the hydrogen in position 5 for the 2.711 mT doublet. The additional 0.076 mT quartet splitting is due to three of the four remaining ring hydrogen atoms.

Increasing the temperature did not result in significant changes of the spectral pattern but for a remarkable progressive decrease of the intensity, the EPR signal being eventually undetectable above −30 °C.

When a small amount of 2-methyl-2-nitrosopropane (MNP) was added to the system, the spectrum shown in Figure 3b was instead observed. This is attributed[23,24] to nitroxide **1c** resulting from the trapping of **1a** by MNP (see Scheme 5).

The low-temperature ($T = -70$ °C) photolysis of a solution of **2** in cyclopropane/toluene containing hexabutylditin led to the observation of an EPR spectrum consisting of a doublet of doublets that could not be attributed to radical **2a**, for which a spectrum similar to that exhibited by **1a** was expected. We believe this spectrum to be due to a rearranged radical and, due to the nature of the isolated products, we tentatively identify this new species as radical **2e**, in which the large doublet would be due to the hydrogen in position 4′ and the smaller one to either of the two hydrogen atoms of the 6′-methylenic group. As was the case for **1**, increasing the temperature led to the disappearance of the EPR signal. In the available temperature interval, an increase of the smaller splitting and a decrease of the larger one were observed when increasing the temperature.

Despite the fast rearrangement process undergone by radical **2a**, the photolysis of **2** in the presence of MNP led to a strong signal from **2c**, a nitroxide structurally related to that observed with sugar **1** (see Table 2 for spectral parameters). The only difference here was the presence of a line-width alternation effect due to hindered rotation around the nitrogen–C6 bond that causes an exchange of the two methylenic hydrogen splittings. Through a careful simulation of the spectral pattern, a value of approximately $1 \times 10^8\ s^{-1}$ for the exchange rate constant could be estimated.

Sugar **3** behaved similarly to sugar **2** in all respects. Its photoreaction with hexabutylditin did not lead to the observation of radical **3a**, but to a spectrum consisting again of a doublet of doublets, attributed to the rearranged radical **3e** (Scheme 6), that exhibited a temperature dependence similar to that observed for **2e**. Nitroxide **3c** was similarly formed when the photoreaction was carried out in the presence of MNP, but in this case the exchange rate constant was faster (ca. $4 \times 10^8\ s^{-1}$). Furthermore, **3c** was accompanied by another nitroxide (**3f**); although the trapping of the rearranged tertiary radical **3e** might have been expected, the spectral parameters of **3f** suggest the trapping of a secondary carbon-centred radical.

Like **1**, and at variance with **2** and **3**, when sugar **4** was photoreacted with hexabutylditin at low temperature it led to the

Table 2. EPR spectral parameters for the radicals observed in the photoreactions of sugars **1**–**4** with hexabutylditin in the absence or in the presence of MNP.

Radical	Hyperfine splitting constants [mT]	*g* factor	*T* [°C]
1a	2.414 (2H), 2.711 (1H), 0.076 (3H)	2.0025(9)	−70
1c	0.071 (1H), 0.734 (1H), 1.256 (1H), 1.501 (1N)	2.0060(7)	23
2e	0.683 (1H), 3.515 (1H)	2.0030(6)	−70
2c	0.0550 (1H), 0.499 (1H), 1.529 (1H), 1.510 (1N)	2.0062(0)	23
3e	0.580 (1H), 3.835 (1H)	2.0031(4)	−70
3c	0.423 (1H), 1.297 (1H), 1.486 (1N)	2.0061(2)	23
3f	0.251 (1H), 1.401 (1N)	2.0061(0)	23
4a	0.112 (1H), 2.253 (2H), 2.399 (1H)	2.0024(3)	−70
4c	0.055 (1H), 0.499 (1H), 1.529 (1H), 1.510 (1N)	2.0061(7)	23

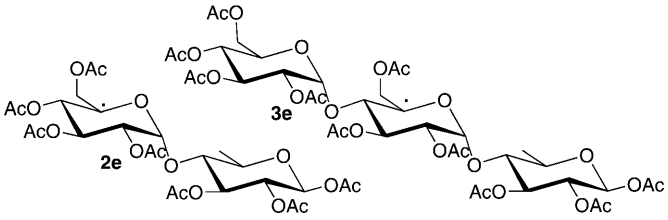

Scheme 6. Rearranged radicals **2e** and **3e**.

detection of radical **4a** (see Table 2). As was the case for **1**, no rearranged radical could be detected. Also the spin-trapping behaviour of **4** paralleled that of **1**, affording nitroxide **4c**, the spectrum of which exhibited exchange between the methylenic hydrogen atoms ($k \approx 8.5 \times 10^6\ s^{-1}$).

Discussion

Relevant mechanistic considerations based on the cyclic voltammetry and EPR studies rationalise the formation of all the known and unknown products involved in the preparative electrolysis of **1**–**4**.

The electroreduction of **1** and **4** afforded the 6,6-dimers **5** and **17**, along with the reduction products **6** and **18**, respectively (see Schemes 7 and 8). The first reduction wave falls at a similar potential for the two derivatives, and corresponds to the formation of their radical anions, which quickly undergo loss of an iodide anion, thereby affording the corresponding primary radicals **1a** and **4a**. As already observed by other authors, the reduction potential is slightly shifted towards more negative values, as the potential scan rate is increased.[25] In the case of **1** and **4**, the second wave is attributed to reduction of radicals **1a** and **4a** to the corresponding carbanions **1b** and **4b**. Thus, on a qualitative basis, the low intensity of the second waves at lower scan rates observed for **1** and **4** is attributed to rapid dimerisation of **1a** and **4a** to form dimers **5** and **17**.

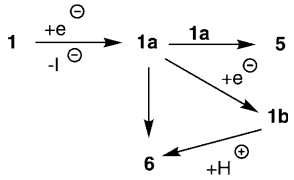

Scheme 7. Mechanism of formation of **5** and **6** following electroreduction of **1**.

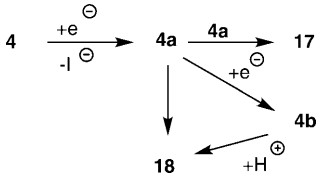

Scheme 8. Mechanism of formation of **17** and **18** following electroreduction of **4**.

The electroreduction of **2** and **3** afforded the 5′,5′-dimeric compounds **8** and **13**, respectively, along with the disproportionation products **9**, **10** and **14**, **15** and of the 6,6-dimers **7** and **12**, respectively (see Schemes 9 and 10). The isolation of

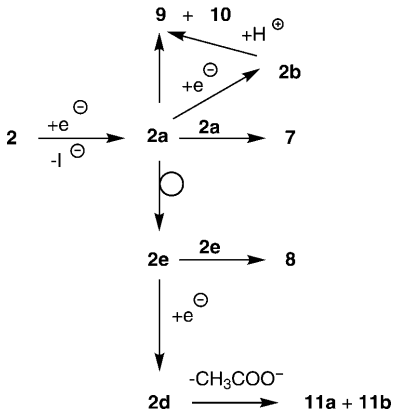

Scheme 9. Mechanism of formation of **7**–**11** following electroreduction of **2**.

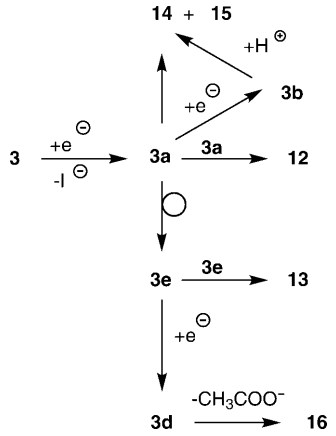

Scheme 10. Mechanism of formation of **12**–**16** following electroreduction of **3**.

these 5′,5′-dimers clearly indicates the occurrence of a rearrangement of the initially formed primary radicals **2a** and **3a** to the corresponding isomers **2e** and **3e**. The maintenance of the C5′ D-glucose configuration in **8** and **13** indicates that **2e** and **3e** remain in an sp^3 orbital, thus affording only one product with their dimerisation. In addition, the isolation of **11a** and **11b** confirms the rearrangement of **2a** to **2e**, further reduced to the carbanion **2d**, followed by acetate anion elimination. Similarly **3e**, reduced to **3d**, eliminates acetate anion to afford **16**.

The different chemical behaviour of **2** and **3** with respect to that of **1** and **4**, was also paralleled by different voltammetric behaviour (see Figure 1). The first wave is still to be associated with the formation of the radical anions of the starting compounds, whereas the second wave, almost invisible at low scan rate, is due to the reduction of radicals **2a** and **3a** to the carbanions **2b** and **3b**. The third wave at

more negative potential is instead believed to reflect the further reduction of the rearranged radicals **2e** or **3e** to the carbanions **2d** or **3d**. Of course, as the scan rate grows, so does the intensity of the second wave, with the reduction of **2a** or **3a** competing more favourably with the rearrangement to **2e** or **3e**.

Radical **1a** could be observed and characterised (see Table 2) by means of EPR spectroscopy upon photolysis at low temperature of a solution of iodosugar **1** in the presence of hexabutylditin. As the temperature was raised, the spectral intensity decreased until complete disappearance of the signal above −30 °C.

Again, we attribute this to the dimerisation process becoming fast enough to lower the steady-state concentration of **1a** below the instrumental detection threshold. If, on the other hand, an efficient spin trap (for example, MNP) is added to the solution, radical **1a** is scavenged before being able to dimerise even at room temperature and nitroxide **1c** is readily observed. It should be noted that the rate constants for the trapping of most carbon-centred radicals by MNP fall in the range between 10^6 and $10^7\,M^{-1}s^{-1}$.[26] The magnetic non-equivalence of the two methylenic hydrogen atoms in nitroxide **1c** might be explained in two ways. The first is that the two hydrogen atoms, being adjacent to a chiral centre, are diastereotopic and hence magnetically different under all conditions. As an alternative, the difference of the two methylenic hydrogen atoms might be explained admitting a hindered, actually almost frozen-out rotation of the *tert*-butylnitroxyl fragment about the newly formed carbon–nitrogen bond. In the case of nitroxide **1c**, we do not see any way to discriminate between these two possibilities. The situation is somehow different for nitroxides **2c**, **3c** and **4c** in the spectra in which line-width alternation effects are clearly evident. For two diastereotopic hydrogen atoms to give rise to line-width alternation, their molecule must exchange between two conformations corresponding to two energy minima, each corresponding to different values of the hydrogen coupling constants; each hydrogen would then exchange with itself and the line-width broadening would result from this difference. The fact that the first and last line of the spectra do not broaden suggests that the variation of the couplings of one hydrogen is exactly counterbalanced by that of the other hydrogen, and in a limiting situation two isomers should be detected. It seems to us more likely that the line-width alternation observed in the spectra of **2c**, **3c** and **4c** is due to the above-mentioned rotation of the *tert*-butylnitroxyl fragment about the N–C6 bond. Indeed, it seems unsurprising to us that such rotation is blocked in **1c**, in which the sugar fragment is a three-fused-ring rigid moiety that may cause severe hindrance to rotation and conformational change. As for **2c**, **3c** and **4c**, the conformational freedom might facilitate the rotation despite the larger size of the sugar moiety, and it would appear that the location of the methylenic group, that is, on the reducing end or non-reducing end of the sugar, may significantly affect this rotation.

The voltammetric behaviour of **4** parallels that of **1**, and does not deserve special comment. Also, the EPR spectrum observed when photolysing at low temperature a solution of **4** containing Bu_6Sn_2 was formally similar to that of **1a**, and consistent with the formation of the corresponding primary radical **4a**. Besides, although photolysis of **4** at room temperature did not lead to the observation of any EPR spectroscopic signal, as it was the case for **1**, the spectrum of the nitroxide **4c** (see Table 2) resulting from the trapping of **4a** was observed in the presence of MNP.

The failure to observe the EPR spectra of radicals **2a** and **3a** when photolysing **2** and **3** at low temperature in the presence of Bu_6Sn_2 seems consistent with a rapid rearrangement of these species taking place and is in line with the aforementioned mechanism (Schemes 9 and 10) suggested to account for the isolation of 5,5-dimers from both sugars. Although the observed spectra have been attributed to the rearranged radicals **2e** and **3e**, the tentative assignment is mainly based on the nature of the isolated products, the spectral parameters being also consistent with other radicals of different structure. Despite their possibly fast rearrangement, the primary radicals **2a** and **3a** are nevertheless trapped by MNP to give nitroxides **2c** and **3c** that are structurally similar to those afforded by halo sugars **1** and **4**. It is also worth noting that MNP does not apparently trap the rearranged radicals **2e** and **3e**, although the spectra of the resulting di-*tert*-alkyl nitroxides might in principle be hidden by the intense signal of di-*tert*-butyl nitroxide (see Figure 2b), a species always present in the photoreactions involving MNP.

Conclusion

Electroreduction of halo sugars on silver cathodes provided synthetic mixed O/C-malto-oligosaccharides: for example, three maltotetraose and two maltohexaose mimics coming from CH_2I reducing and non-reducing end-unit precursors, characterised by a central interglycosydic carbon–carbon bond instead of the usual O-glycosidic linkage present in natural and a large part of synthetic oligosaccharides.

Experimental Section

Materials: All commercially available reagents, including dry solvents, were used as received. Organic extracts were dried over sodium sulfate, filtered and concentrated under vacuum by using a rotary evaporator. All compounds were dried under high vacuum. Reactions were monitored by thin-layer chromatography on precoated Merck silica gel 60 F254 plates and visualised by staining with 10% H_2SO_4 in water and with a solution of cerium sulfate (1 g) and ammonium heptamolybdate tetrahydrate (27 g) in water (469 mL) and concentrated sulfuric acid (31 mL). Flash chromatography was performed on Fluka silica gel 60.

Analytical equipment and characterisation methods: Melting points were measured with a 10× magnification Reichert microscope equipped with a heating plate and are not corrected. Optical rotations were measured using a Dr. Kernichen Propol digital automatic polarimeter.

^{1}H and ^{13}C NMR spectra were recorded at 303 K using Bruker Avance 500 and 600 spectrometers equipped with a 5 mm 1H/X inverse probe and with a TCI cryoprobe, respectively. Assignments were made through HMQC, COSY and TOCSY experiments.

Analysis was made by means of ESI-Q-TOF mass spectrometry. The acquisitions were performed by direct infusion of the sample solution (prepared at the appropriate concentration in CH_3CN) sprayed at 4 μL min^{-1} in the ionisation source of an ESI-Q-TOF mass spectrometer (Bruker Daltonics) operating in positive mode on the mass range from *m*/*z* 50 to 2000 (instrumental conditions: capillary voltage 4500 V, nebuliser gas 0.4 bar, dry gas 4.0 L min^{-1}, dry temperature 180 °C). Mass calibration was performed using sodium formate clusters.

Analytical HPLC were performed using a Hypersil Column BDS C18 (250×4.6 mm). Rheodine valve volume: 20 μL. Eluent: 55:45 acetonitrile/water. Flow rate: 1.5 mL min^{-1}. UV detection at 210 nm. Samples were dissolved in acetonitrile at the concentration of 1 mg mL^{-1}; 20 μL were injected. Semi-preparative HPLC was performed under the same conditions using an Hypersil BDS C18 250×10 mm column from Thermo Hypersil, a Rheodine valve of 100 μL and a flow rate of 5 mL min^{-1}. Samples were dissolved in acetonitrile at the concentration of 50–100 mg mL^{-1}; 70–100 μL were injected.

EPR equipment and methods: EPR spectra were recorded by means of an upgraded ER200D-ESP300 Bruker X-band EPR spectrometer operating at a frequency of approximately 9.3 GHz. The spectrometer was equipped with a standard variable temperature accessory, a dedicated computer for the storage and manipulation of data, an NMR spectroscopic gaussmeter for the calibration of the magnetic field and a frequency counter for the determination of *g* factors that were corrected with respect to the value of perylene radical cation in concentrated sulfuric acid (2.0025_8). In a typical experiment, a thoroughly degassed solution of the halo sugar and of hexabutylditin in cyclopropane (THF or toluene) was cooled at the desired temperature inside the cavity of the spectrometer and irradiated with the unfiltered light of a 1 kW high-pressure mercury lamp. For spin-trapping experiments, a very small amount of MNP was also added to the sample. Typical instrumental settings were as follows: modulation amplitude 0.025 mT, receiver gain 1×10^5, power 1 mW, scan width 10 mT. The experimental spectra were computer simulated using custom-made software based on a Monte Carlo minimisation procedure.[27]

Synthesis of starting iodosugars 2–4: Compounds **2** and **4** were prepared according to literature procedures and had melting points and spectral data in agreement with those reported in the literature. Compound **3** was characterised by ^{1}H and ^{13}C NMR spectra as they are not present in the literature.

Acetobromomaltose and acetobromomaltotriose were prepared from commercial maltose monohydrate and maltotriose.[28]

They were converted to the corresponding peracetylated 1,6-anydromaltose and 1,6-anydromaltotriose, precursors of the peracetylated 6-formyl-maltose and 6-formyl-maltotriose, respectively.[19] Iodination of the peracetylated 6-hydroxyl-maltose and 6-hydroxylmaltotriose, coming from the formyl group hydrolysis, afforded **2** and **3**, respectively.[29]

Maltose was first protected as 4′,6′-benzylidene maltose and was then fully acetylated. Debenzylation gave peracetylated 4′,6′-hydroxyl maltose, which was protected at the 6′-position with the trityl group and acetylated at the 4′-position.[30] After detritylation, 6′-hydroxyl peracetylated maltose was iodinated to **4**.[29]

Compound 3: ^{1}H NMR (500 MHz, $CDCl_3$; the three rings are termed A, B and C for convenience, with ring C bearing I): $\delta=2.14$–1.98 (s; C*H*$_3$CO), 3.37 (dt, $J_1=3.4$ Hz, $J_2=9.2$ Hz, 1H), 3.47 (dd, $J_{6aC,5C}=4.0$ Hz, $J_{6aC,6bC}=11.3$ Hz; H-6aC), 3.61 (dd, $J_{6bC,5C}=3.2$, $J_{6bC,6aC}=11.3$ Hz; H-6bC), 3.89–3.98 (m, 4H), 4.02 (dd, $J_1=2.6$ Hz, $J_2=12.5$ Hz, 1H), 4.21 (dd, $J_1=3.5$ Hz, $J_2=12.3$ Hz, 1H), 4.23 (dd, $J_1=3.0$ Hz, $J_2=12.3$ Hz, 1H), 4.57 (dd, $J_1=1.9$ Hz, $J_2=12.3$ Hz, 1H), 4.73 (dd, $J_{2B,1B}=4.0$ Hz, $J_{2B,3B}=10.3$ Hz; H-2B), 4.84 (dd, $J_{2A,1A}=4.0$ Hz, $J_{2A,3A}=10.6$ Hz; H-2A), 4.94 (dd, $J_{2C,1C}=8.0$ Hz, $J_{2C,3C}=8.9$ Hz; H-2C), 5.04 (t, $J_{4A,3A}=9.8$ Hz, $J_{4A,5A}=9.8$ Hz; H-4A), 5.27–5.39 (m, 5H), 5.80 ppm (d, $J_{1C,2C}=8.0$; H-1C); ^{13}C NMR (125 MHz, CDCl3): $\delta=7.2$ (*C*H$_2$I), 21.2–21.6 (*C*H$_3$CO), 62.1, 63.7, 68.7, 69.2, 70.0, 70.1, 71.0, 71.7, 72.4, 73.1, 75.5, 91.5, 96.3, 96.4, 169.6–171.2 ppm (CH$_3$*C*O).

Electrochemical equipment and general procedures: Cyclic voltammetry and preparative electrolysis experiments were carried out using an Amel 2053 potentiostat coupled with an Amel 7800 interface (electrochemical measurements managing software Junior Assist). Supporting electrolyte: tetraethylammonium tetrafluoborate (TeaTfb). Solvent: commercial anhydrous acetonitrile. Electrodes: reference saturated calomel electrode (SCE), silver cathode (2 mm diameter) and platinum wire (cyclic voltammetry), cathode and anode silver plates 1 cm×3 cm (preparative electrolysis). Cells: 50 mL homemade flask (cyclic voltammetry), sintered glass diaphragm two-compartment cell (preparative electrolysis).

Cyclic voltammetry experiments: Cyclic voltammetry experiments were run at 20 °C in a thermostat-controlled cell with 5 mM iodosugar. Tetraethylammonium tetrafluoborate (TeaTfb; 0.1 M) was used as supporting electrolyte, in anhydrous acetonitrile with silver cathode, platinum anode and SCE (saturated calomel electrode) as reference electrode.

Preparative electrolysis experiments: All the electrolyses were run in a two-compartment cell, the anode and cathode being divided by a glass frit. Cathode and anode were both silver plates, and the anode and cathode electrolyte solutions consisted of TeaTfb (0.1 M) in anhydrous acetonitrile, and were briefly pre-electrolysed between −1.3 and −2.2 V until the obtainment of a low and constant current intensity. After pre-electrolysis, iodosugar was added to the cathode solution and extensively electrolysed under N_2 in potentiostatic conditions on the base of voltammetric measurements.

Electrolysis of 2: After pre-electrolysis, **2** (1.76 g, 2.46 mmol) was added to the cathode solution (70 mL) and exhaustively electrolysed under N_2 at −1.35 V (5 h) and at −1.45 V (1 h). The solution at the cathode compartment was concentrated and precipitated with AcOEt. The solid supporting electrolyte was filtered off. The filtrate was evaporated at reduced pressure and the residue was subjected to flash chromatography on silica gel with a gradient of hexane/ethyl acetate. A ratio of 4:6 hexane/acetate is sufficient to elute and separate **9**, **10**, **11a** and **11b**, whereas the elution of pure **7** and **8** needs a 3:7 ratio.

Electrolysis of 3: After pre-electrolysis, **3** (300 mg, 0.29 mmol) was added to the cathode solution (10 mL) and exhaustively electrolysed under N_2 at −1.30 V (3 h). The solution at the cathode compartment was concentrated and precipitated with AcOEt. The solid supporting electrolyte was filtered off. The filtrate was evaporated at reduced pressure and the residue was subjected to flash chromatography on silica gel with a gradient of hexane/ethyl acetate. A gradient from 1:1 to 3:7 eluted **14**, **15** and **16**. A further gradient from 2:8 to 1:9 was necessary to elute **12** and **13** in mixture. The mixture of **12** and **13** was separated by semi-preparative HPLC.

Electrolysis of 4: After the pre-electrolysis, **4** (200 mg, 0.27 mmol) was added to the cathode solution (10 mL) and was exhaustively electrolysed under N_2 at −1.30 V (1 h) and at −1.35 V (2 h). The solution at the cathode compartment was concentrated and precipitated with AcOEt. The solid supporting electrolyte was filtered off. The filtrate was evaporated at reduced pressure and the residue was subjected to flash chromatography on silica gel (3:7 hexane/acetate) to separate the more polar **17** from the less polar **18**.

1,2,3,2′,3′,4′,6′-Hepta-*O*-acetyl-6-deoxy-α-maltos-6-yl dimer (7): M.p. 165–166 °C; $[\alpha]_D=+98.2$ ($c=1$ in CH_3Cl); ESI-Q-TOF MS: *m*/*z* calcd for $C_{52}H_{70}O_{34}Na_1$: 1261.3641; found: 1261.3602 $[M+Na]^+$.

1,2,3,2′,3′,4′,6′-Hepta-*O*-acetyl-6-deoxy-6-methyl-α-maltos-5′-yl dimer (8): M.p. 172–173 °C; $[\alpha]_D=+112.6$ ($c=1$ in $CHCl_3$); ESI-Q-TOF MS: *m*/*z* calcd for $C_{52}H_{70}O_{34}Na_1$: 1261.3641; found: 1261.3631 $[M+Na]^+$.

1,2,3,2′,3′,6′,2″,3″,4″,6″-Deca-*O*-acetyl-6-deoxy-α-maltotrios-6-yl dimer (12): ESI-Q-TOF MS: *m*/*z* calcd for $C_{76}H_{102}O_{50}Na_1$: 1837.5331; found: 1837.5390 $[M+Na]^+$.

1,2,3,2′,3′,6′,2″,3″,4″,6″-Deca-*O*-acetyl-6-deoxy-6-methyl-α-maltotrios-5′-yl dimer (13): M.p. 148–149 °C; $[\alpha]_D=+124.3$ ($c=1$ in CH_3Cl); ESI-Q-TOF MS: *m*/*z* calcd for $C_{76}H_{102}O_{50}Na_1$: 1837.5331; found: 1837.5401 $[M+Na]^+$.

Table 3. NMR spectroscopic characterisation of new mixed O/C-maltotetraose and -maltohexaose mimics **7**, **8**, **12**, **13** and **17**.[a]

	7			**8**			**12**			**13**			**17**		
	^{1}H		^{13}C	^{1}H		^{13}C	^{1}H		^{13}C	^{1}H		^{13}C	^{1}H		^{13}C
	δ	J	δ	δ	J	δ	δ	J	δ	δ	J	δ	δ	J	δ
H/C-1A	5.64	4.1	98.0	5.42	3.5	100.4	5.663	3.9	99.0	5.58	4.3	100.2	5.312	3.8	95.6
H/C-2A	5.10	10.6	73.5	5.41	8.7	73.3	5.15	10.7	73.4	5.32	9.5	72.8	4.77	10.5	70.6
H/C-3A	5.93	9.7	72.2	6.01	9.8	71.6	5.99	9.7	72.4	5.71	9.5	73.6	5.277	9.8	69.6
H/C-4A	5.49	10.1	71.3	6.04	–	72.2	5.43	9.7	71.6	5.46	9.6	70.6	4.82	9.8	70.5
H/C-5A	4.25	2.2	71.7	–	–	76.8	4.51	2.4	71.87	4.53	2.5	72.5	–	–	69.0
		3.5						3.4			2.8				
H/C-6A	4.32	12.0	64.7	4.30	12.6	66.4	4.43	12.2	64.5	4.43	12.7	63.8	1.61	n.d.	23.4
	4.73			5.22			4.48			4.50			1.67		
H/C-1 B	5.73	8.5	94.7	5.93	8.3	94.7	5.64	4.1	97.4	5.69	3.5	100.3	5.78	8.1	91.4
H/C-2 B	5.13	9.4	74.7	5.35	9.3	74.3	4.90	10.5	73.9	5.21	8.8	73.4	4.98	8.1	71.1
H/C-3 B	5.45	9.2	78.7	5.48	9.0	76.4	5.93	9.0	75.4	5.81	8.6	75.8	5.302	9.1	75.0
H/C-4 B	3.61	9.2	77.9	3.38	10.3	84.9	4.18	9.7	75.0	5.08	–	79.4	3.94	9.1	73.1
H/C-5 B	2.74	n.d.	76.9	3.54	5.0	75.2	4.28	2.4	71.81	–	–	76.9	3.86	2.4	73.2
								4.1							
H/C-6 B	1.63	n.d.	30.6	1.59	–	20.3	4.61	12.3	66.3	4.60	12.0	66.4	4.14	12.2	63.2
	1.67						4.82			5.49			4.43		
H/C-1 C	–	–	–	–	–	–	5.89	9.5	95.3	5.99	8.4	94.7	–	–	–
H/C-2 C	–	–	–	–	–	–	5.24	9.5	74.8	5.38	9.4	74.5	–	–	–
H/C-3 C	–	–	–	–	–	–	5.665	9.2	78.8	5.52	9.2	77.4	–	–	–
H/C-4 C	–	–	–	–	–	–	3.73	9.2	77.8	3.62	–	84.3	–	–	–
H/C-5 C	–	–	–	–	–	–	3.07	>10.0	78.0	3.60	–	74.7	–	–	–
								2.8							
H/C-6 C	–	–	–	–	–	–	1.72	n.d.	23.2	1.63	–	20.6	–	–	–
							1.87								
A/B/C $Me_{O-acetyl}$	1.7–2.1	–	22–24	1.6–2.3	–	22–24	1.6–1.9	–	22–24	1.6–2.4	–	22–24	1.8–2.2	–	22–24

[a] Chemical shifts (δ) in ppm; coupling constants (J) in Hz; n.d. = not determined.

1,2,3,6,2′,3′,4′-Hepta-*O*-acetyl-α-maltos-6′-yl dimer (17): M.p. 121–122 °C; $[\alpha]_D = +158.2$ ($c = 1$ in CH_3Cl); ESI-Q-TOF MS: m/z calcd for $C_{52}H_{70}O_{34}Na_1$: 1261.3641; found: 1261.3638 $[M+Na]^+$.

Table 3 reports full details of the NMR spectroscopic characterisation of **7**, **8**, **12**, **13** and **17** in C_6D_6. As concerns compounds **8** and **13**, the NMR spectroscopy $^3J_{2B,3B}$ and $^3J_{3B,4B}$ coupling constant values of the ring involved in C5′–C5′ bonds indicate the maintenance of the original $^4C_1$ ring conformation. In addition, the $[\alpha]_D$ values support a maintenance of the C5′ D-glucose configuration, instead of the possible epimerisation of this residue to the L-ido configuration. In fact, $[\alpha]_D$ values of the tetramers increase from +63.0, the original value of β-octaacetylmaltose, to +98.2 for **7**, due to the effect of chain elongation, and up to +112.6 for tetra-**8**. Whereas for the hexasaccharides, the $[\alpha]_D$ value of +86 for β-undecaacetylmaltotriose increases to +124.3 for **13**.

Compound 11a: ^{1}H NMR (500 MHz, $CDCl_3$; the two rings are termed A and B for convenience, exocyclic double bond between 5′ and 6′ in A): $\delta = 1.28$ (d, $J_{6B,5B} = 6.1$ Hz; CH_3, H-6B), 1.98–2.11 (s; CH_3CO), 3.60 (m; H-5B), 3.71 (t, $J_{4B,3B} = J_{4B,5B} = 9.1$ Hz; H-4B), 4.50 (t, $J_{6aA,6bA} = 2.0$ Hz, $J_{6aA,4A} = 1.8$ Hz; H-6aA), 4.67 (t, $J_{6bA,6aA} = 2.0$ Hz, $J_{6bA,4A} = 1.8$ Hz, H-6bA), 4.83 (dd, $J_{1A,2A} = 3.8$ Hz, $J_{3A,2A} = 10.0$; H-2A), 4.89 (t, $J_{1B,2B} = J_{3B,2B} = 9.2$ Hz; H-2B), 5.18 (t; H-3B), 5.33 (t, $J_{3A,4A} = 10.0$ Hz; H-3A), 5.42 (dd; H-4A), 5.42 (d; H-1A), 5.64 ppm (d, $J_{1B,2B} = 8.2$ Hz; H-1B); ^{13}C NMR (125 MHz, $CDCl_3$): $\delta = 18.9$ (C-6B), 19.4–21.8 (CH_3CO), 68.2 (C-3A), 68.6 (C-4A), 69.8 (C-2A), 71.2 (C-2B), 71.6 (C-5B), 75.5 (C-3B, C-4B), 91.2 (C-1B), 95.2 (C-1A), 97.9 (C-6A), 150.8 (C-5A), 169.1–170.4 ppm (CH$_3$CO); ESI-Q-TOF MS: m/z calcd for $C_{24}H_{32}O_{15}Na_1$: 583.1633; found: 583.1689 $[M+Na]^+$.

Compound 11b: ^{1}H NMR (500 MHz, $CDCl_3$, the two rings are termed A and B for convenience, endocyclic double bond between 4′ and 5′ in A): $\delta = 1.22$ ($J_{6B,5B} = 6.1$ Hz; CH_3, H-6B), 1.98–2.11 (s; CH_3CO), 3.55 (m, 1H; H-5B), 3.64 (t, $J_{4B,3B} = J_{4B,5B} = 9.3$ Hz; H-4B), 4.41 (d, $J_{6aA,6bA} = 13.3$ Hz, 1H; H-6aA), 4.37 (d, $J_{6bA,6aA} = 13.3$ Hz, 1H; H-6bA), 4.87 (dd, $J_{1A,2A} = 3.0$ Hz, $J_{3A,2A} = 8.6$ Hz, 1H; H-2A), 4.89 (t, $J_{1B,2B} = J_{3B,2B} = 9.2$ Hz, 1H; H-2B), 4.95 (d, $J = 2.2$ Hz, 1H; H-4A), 5.22 (t, $J = 9.3$ Hz, 1H; H-3B), 5.38 (d, 1H; H-1A), 5.44 (d, 1H; H-3A), 5.62 ppm (d, $J_{1B,2B} = 8.4$ Hz, 1H; H-1B); ^{13}C NMR (125 MHz, $CDCl_3$): $\delta = 17.3$ (C-6B), 19.4–21.8 (CH_3CO), 62.0 (C-6A), 69.3 (C-2A), 71.2 (C-5B, C-2B), 75.0 (C-3B), 76.3 (C-4B), 93.6 (C-1B), 95.4 (C-1A), 99.3 (C-4A), 169.1–170.4 ppm (CH$_3$CO); ESI-Q-TOF MS: m/z calcd for $C_{24}H_{32}O_{15}Na_1$: 583.1633; found: 583.1690 $[M+Na]^+$.

Compound 16: ^{1}H NMR (500 MHz, $CDCl_3$, the three rings are termed A, B and C for convenience): $\delta = 1.36$ (d, $J_{6C,5C} = 6.1$ Hz; CH_3, H-6C), 1.90–2.20 (m; CH_3CO), 3.664 (m, $J_{6C,5C} = 6.1$ Hz; H-5C), 3.757 (dd, $J_{4C,5C} = J_{4C,3C} = 9.2$ Hz; H-4C), 4.090 (m; H-5A), 4.109 (m, $J_{6bA,5A} = 2.4$ Hz; H-6bA), 4.154 (dd, $J_{6aA,5A} = 4.9$ Hz, $J_{6aA,6bA} = 12.6$ Hz; H-6aA), 4.280 (dt, $J_{4B,3B} = 9.4$ Hz, $J_{4B,6B} = 1.5$ Hz; H-4B), 4.767 (dd, $J_{2B,\ 1B} = 3.8$ Hz, $J_{2B,3B} = 10.4$ Hz; H-2B), 4.788 (dd, $J_{2A,1A} = 3.8$ Hz, $J_{2A,\ 3A} = 10.8$ Hz; H-2A), 4.840 (t, $J_{6aB,4B} = 1.5$ Hz; H-6aB), 4.946 (dd, $J_{2C,3C} = 9.3$ Hz, $J_{2C,1C} = 8.4$ Hz; H-2C), 5.012 (t, $J_{4A,5A} = J_{4A,3A} = 9.8$ Hz; H-4A), 5.027 (t; H-6bB), 5.214 (dd, $J_{2C,3C} = J_{3C,4C} = 9.3$ Hz; H-3C), 5.363 (t, $J_{2B,3B} = J_{3B,4B} = 9.8$ Hz; H-3B), 5.378 (d, $J_{1A,2A} = 3.7$ Hz; H-1A), 5.417 (d, $J_{1B,2B} = 3.6$ Hz; H-1B), 5.448 (dd, $J_{2A,3A} = J_{3A,4A} = 9.8$ Hz; H-3A), 5.69 ppm (d, $J_{2C,1C} = 8.4$ Hz; H-1C); ^{13}C NMR (125 MHz, $CDCl_3$): $\delta = 19.3$ (C-6C; CH_3), 20.0–21.5 (CH_3CO), 61.47 (C-6A), 68.03 (C-4A), 68.47 (C-5A), 69.24 (C-3A), 70.08 (C-3B), 70.158 (C-2B), 70.359 (C-2A), 71.26 (C-2C), 71.7 (C-5C), 71.99 (C-4B), 75.34 (C-3C), 75.68 (C-4C), 91.09 (C-1C), 95.30 (C-1A), 91.50 (C-1B), 95.7 (C-1C′), 99.97 (C-6B, C=CH_2), 150.99 (quaternary C-5B, C=CH$_2$), 169.0–170.6 ppm (CH$_3$CO); ESI-Q-TOF MS: m/z calcd for $C_{36}H_{48}O_{23}Na_1$: 871.2479; found 871.2497 $[M+Na]^+$. Quaternary C-5B shows in the HMBC spectrum correlation peaks with H-3B, H-1B, H-6aB, H-6bB and H-4B. In the HMBC spectrum, H-1C shows a correlation peak with C-O, H-1B shows with C-4C, H-4B with C-1A.

Acknowledgements

The authors would like to acknowledge partial financial support from Fifth Framework Programme (FP5)/Quality of Life and Management of

Living Resources, contract nos. QLK3-CT-2002-02049 ("Heparanase Inhibitors in Antiangiogenic and Antimetastatic Cancer Therapy") and MIUR-FIRB2001 ("Glycosaminoglycans Elastase and Selectins Antagonist as Anti-Inflammatory Drugs"). We also thank Dr. Roberto Santarsiero, Dr. Marco Guerrini and Dr. Sara Guglieri of the Ronzoni and NMR Centre staff, as well as Dr. Stefano Elli and Dr. Daniel Pizzolato of "G. Natta" for their contribution to the Experimental Section.

[1] A. Alberti, M. A. Della Bona, D. Macciantelli, F. Pelizzoni, G. Sello, G. Torri, E. Vismara, *Tetrahedron* **1996**, *52*, 10241–10248.
[2] M. Guerrini, G. Torri, P. R. Mussini, S. Rondinini, E. Vismara, *Chem. Commun.* **1998**, 1575–1576.
[3] S. Rondinini, P. R. Mussini, G. Sello, E. Vismara, *J. Electrochem. Soc.* **1998**, *145*, 1108–1112.
[4] A. Alberti, S. Bertini, M. Comoli, M. Guerrini, A. Mele, E. Vismara, *Tetrahedron* **2000**, *56*, 6291–6297.
[5] M. Guerrini, S. Guglieri, R. Santarsiero, E. Vismara, *Tetrahedron: Asymmetry* **2005**, *16*, 243–253.
[6] A. Imberty, S. Peréz, *Chem. Rev.* **2000**, *100*, 4567–4588, and references therein.
[7] a) C. R. Parish, C. Freeman, K. J. Brown, D. J. Francis, W. B. Cowden, *Cancer Res.* **1999**, *59*, 3433–3441; b) C. R. Parish, W. B. Cowden, Patent US006143730A.
[8] H. Gong, M. R. Gagne, *J. Am. Chem. Soc.* **2008**, *130*, 12177–12183.
[9] a) J. P. Carver, *Pure Appl. Chem.* **1993**, *65*, 763–770; b) P. K. Qasba, *Carbohydr. Polym.* **2000**, *41*, 293–309.
[10] A. Laederach, P. J. Reilly, *Proteins Struct. Funct. Bioinf.* **2005**, *60*, 591–597, and references therein.
[11] M. Seo, N. Castillo, R. Ganzynkowicz, C. R. Daniels, R. J. Woods, T. L. Lowary, P.-N. Roy, *J. Chem. Theory Comput.* **2008**, *4*, 184–191.
[12] a) R. W. Armstrong, B. R. Teegarden, *J. Org. Chem.* **1992**, *57*, 915–922; b) N. Navarre, A. H. van Oijen, G. J. Boons, *Tetrahedron Lett.* **1997**, *38*, 2023–2026; c) R. Alibés, D. R. Bundle, *J. Org. Chem.* **1998**, *63*, 6288–6301; d) M. C. Galan, A. P. Venot, J. Glushka, A. Imberty, G.-J. Boons, *J. Am. Chem. Soc.* **2002**, *124*, 5964–5973.
[13] J.-F. Espinosa, M. Martìn-Pastor, J. L. Asensio, H. Deitrich, M. Martìn-Lomas, R. Schmidt, J. Jiménez-Barbero, *J. Am. Chem. Soc.* **1996**, *118*, 10862–10871.
[14] a) J. Jimenéz-Barbero, J. L. Asensio, F. J. Cañada, A. Proveda, *Curr. Opin. Struct. Biol.* **1999**, *9*, 549–555; b) J. M. Alonso-Plaza, M. A. Canales, M. Jiménez, J. L. Roldan, A. Garcìa-Herrero, L. Iturrino, J. L. Asensio, F. J. Cañada, A. Romero, H.-C. Siebart, S. Andrè, D. Solìs, H.-J. Gabius, J. Jiménez-Barbero, *Biochim. Biophys. Acta Gen. Subj.* **2001**, *1568*, 225–236; c) A. Canales, J. Angulo, R. Ojeda, M. Bruix, R. Fayos, R. Lozano, G. Gimenez-Gallego, M. Martin-Lomas, P. M. Nieto, J. Jiménez-Barbero, *J. Am. Chem. Soc.* **2005**, *127*, 5778–5779; d) A. Almond, B. O. Petersen, J. Ø. Duus, *Biochemistry* **2004**, *43*, 5853–5863.
[15] E. Vismara, G. Torri, A. Naggi, I. Vlodavsky, Patent Application Number EP08160464, **2008**.
[16] E. Vismara, A. Donna, F. Minisci, A. Naggi, N. Pastori, G. Torri, *J. Org. Chem.* **1993**, *58*, 959–963.
[17] H. P. Wessel, M. Trumtel, R. Minder, *J. Carbohydr. Chem.* **1996**, *15*, 523–548.
[18] K. Takeo, T. Kuge, *Carbohydr. Res.* **1976**, *48*, 282–289.
[19] S. Cottaz, C. Apparu, H. Driguez, *J. Chem. Soc. Perkin Trans. 1* **1991**, 2235–2241.
[20] R. Blattner, R. J. Ferrier, P. Prasit, *Chem. Commun.* **1980**, 944–945.
[21] J. F. Stoddard in *Stereochemistry of carbohydrates.* Wiley-Interscience, New York, **1971**.
[22] F. A. Neugebauer in *Landolt-Börnstein Magnetic properties of free radicals, New Series, Group II, Vol. 17, Part b* (Ed.: H. Fischer), Springer, Berlin, **1987**.
[23] A. R. Forrester in *Landolt-Börnstein Magnetic properties of free radicals. New Series, Group II, Vol. 9, Part c* (Eds.: H. Fischer, K.-H. Hellwege), Springer, Berlin, **1979**.
[24] A. Alberti in *Landolt-Börnstein Magnetic properties of free radicals. New Series, Group II, Vol. 26, Subvolume d* (Ed.: H. Fischer), Springer, Berlin, **2005**.
[25] C. P. Andrieux, I. Gallado, J.-M. Savéant, *J. Am. Chem. Soc.* **1989**, *111*, 1620–1626.
[26] T. J. Kemp, *Prog. React. Kinet. Mech.* **1999**, *24*, 287–358.
[27] M. Lucarini, B. Luppi, G. F. Pedulli, B. P. Roberts, *Chem. Eur. J.* **1999**, *5*, 2048–2054.
[28] I. Damager, C. E. Olsen, B. L. Moller, M. S. Motawia, *Synthesis* **2002**, 418–426.
[29] B. Classon, Z. Liu, B. Samuelsson, *J. Org. Chem.* **1988**, *53*, 6126.
[30] K. Takeo, K. Shinmitsu, *Carbohydr. Res.* **1984**, *133*, 135–145.

Received: March 31, 2009
Published online: July 14, 2009

